Intermetallics 19 (2011) 762–768

Contents lists available at ScienceDirect

Intermetallics

journal homepage: www.elsevier.com/locate/intermet

Recycling of gamma titanium aluminide scrap from investment casting operations

J. Reitz [a,*], C. Lochbichler [b], B. Friedrich [a]

[a] RWTH Aachen University, IME Process Metallurgy and Metals Recycling, Intzestrasse 3, 52056 Aachen, Germany
[b] Formerly IME, Now Voestalpine Giesserei Traisen GmbH, Mariazellerstrasse 75, A-3160 Traisen, Austria

ARTICLE INFO

Article history:
Received 2 November 2010
Accepted 15 November 2010
Available online 13 December 2010

Keywords:
A. Titanium aluminides, based on TiAl
B. Thermodynamic and thermochemical properties
C. melting
C. casting (including segregation)
C. purification

ABSTRACT

In investment casting processes for TiAl alloys, a substantial amount of the original raw material does not end-up as a final product but is instead solidified in runners and feeders of the casting system or as a skull in the crucible. Because of the high prices for the virgin alloys, there is a strong interest in remelting this scrap. This is a challenging task due to the tremendous oxygen affinity of titanium alloys. The contact of the melt with shell mould and crucible material leads to oxygen pickup during casting. Up to now no technique exists to avoid this effect, thus any recycling process for TiAl casting scrap potentially needs a deoxidation technique. Within the IMPRESS project, experimental proof for the feasibility of a novel treatment has been obtained in a series of tests and results are presented in this paper. Casting scrap from pilot-trials has been consolidated via classic vacuum induction melting (VIM) in special ceramic crucibles and then successfully deoxidized by pressure electroslag remelting (PESR) under reactive slags. Further refining by vacuum arc remelting (VAR) finally leads to removal of dissolved reducing agent and impurities like non-metallic-inclusions.

1. Introduction

1.1. The integrated recycling concept

Due to their good corrosion resistance, their low density and interesting mechanical properties at high temperatures γ-phase titanium aluminides are widely regarded as the next generation material for high temperature structural applications in the aerospace and automotive industry. However the high material and production costs for semi-finished products actually slow down an industrial breakthrough to mass production of γ-TiAl.

From a processing standpoint the material yield in investment casting is similar for TiAl as for standard titanium alloy casting with a loss in the range of 40–60%. On the other hand γ-TiAl alloys are produced at a tremendously higher cost compared to classic titanium alloys like Ti-6Al-4 V due to more strict specifications on alloy composition and homogeneity. This is necessary in order to achieve desired high temperature strength at an acceptable level of ductility. Thus material losses during casting of γ-TiAl should have a more severe impact on overall product cost than in classical titanium alloy casting and hence recycling becomes even more economically interesting for γ-TiAl than it is potentially for titanium.

Since the year 2000 a research group at IME, Aachen aims on cost-reduced production methods for γ-TiAl. While one path follows the alternative aluminothermic production of TiAl from TiO_2 pigment and subsequent refining [1,2], parallel activities aim for development of an efficient process for recycling TiAl-scrap from casting operations in order to avoid the present downgrading of this valuable material as an alloying element in the steel industry.

In IME's integrated concept (see Fig. 1), which includes both alternative primary production and recycling, the first melting of a scrap charge is done by conventional vacuum induction melting (VIM) using specialised ceramic lining. This step can include preliminary deoxidation by injection of calcium metal into the melt [3]. Full deoxidation and reactive refining follows during pressure electroslag remelting (PESR) using a continuously re-activated calcium-metal-containing slag. During final vacuum arc remelting (VAR) micron size slag inclusions as well as dissolved calcium and hydrogen can be removed. For each processing step special equipment requirements and metallurgical challenges have to be met and the different refining opportunities need to be exploited to obtain a sound recycled TiAl ingot. This paper presents the latest progress of the work with a special focus on oxygen removal, refining and homogenisation by PESR. Final VAR melting is presently under investigation and results shall be presented in a second publication.

1.2. Introduction to electroslag remelting (ESR)

ESR is widely applied in the production of speciality steels and superalloys nowadays in order to obtain ingots with superior cleanliness, minimized segregation and a homogeneous microstructure.

* Corresponding author. Tel.: +49 2418095196.
E-mail address: jan.reitz@rwth-aachen.de (J. Reitz).

0966-9795/$ – see front matter © 2010 Elsevier Ltd. All rights reserved.
doi:10.1016/j.intermet.2010.11.015

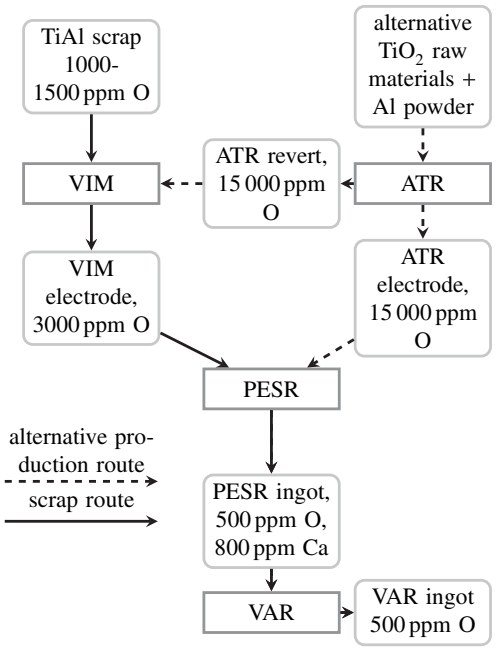

Fig. 1. Integrated concept for alternative production and recycling of TiAl developed at IME, Aachen.

As a basic principle the tip of a consumable electrode, made from the alloy to be refined, is dipped into a molten flux, contained in a water-cooled copper crucible. Electrical currents (most commonly AC) are applied between the electrode and the flux and result in joule heating up to the melting point of the metal. A liquid metal film forms on the downside of the electrode and hence metal droplets are released which sink through the flux bath due to the difference in density. The slag bath floats on a liquid metal pool which collects the droplets. Through cooling at the mould surfaces, solidification occurs and the process continuously builds up a refined ingot with a controlled microstructure and smooth outer surface.

The potentials of the application of ESR for the remelting of pure titanium using CaF_2-based fluxes has been investigated by various researchers [4–10] with promising results concerning the possibility to produce slab-shaped ingots and improvements regarding material yield and energy consumption in comparison to VAR. Results also show interesting possibilities to reduce segregation effects due lower possible melt rates compared to VAR. Mechanical properties of ESR remelted c.p. titanium are reported to be comparable to VAR melted titanium [5], despite an ongoing discussion about possible solution of fluorine in the metal [11].

2. Materials and methods

2.1. Characterisation of raw material

A first evaluation of the process was carried out using spent sputter targets of the binary composition Ti50Al as a starting material of high purity, low initial oxygen content and avoiding effects of ternary alloying elements. As a second step, scraps from casting trials within the IMPRESS project [12] on the alloys Ti-46Al8Nb and Ti46Al8Ta were recycled (Fig. 2).

In the recycling of metallic scrap, sampling of the input material plays an important role. Usually scrap input comes in batches and representative samples have to be prepared and analysed allowing for calculation of an optimum charge in the crucible. Depending on the result of this, the target composition was adjusted by adding titanium sponge, aluminium granules (99.95% purity) and tantalum sheet scraps from stamping operations.

2.2. Consolidation by VIM

Melting trials for consolidation of scrap and casting of electrodes were carried out using a vacuum induction furnace with a melt capacity of 14 l and a nominal melting power of 150 kW. Because of the high reactivity of TiAl melts towards ceramic crucibles, special high purity CaO crucibles were selected (see Section 3.1). Chemical analysis of the crucible material reveals very little contamination by other oxides (SiO_2 0.14 wt%, Al_2O_3 0.07 wt%, Fe_2O_3 0.05 wt%, MgO 0.48 wt%). The crucible volume allowed a charge weight of approximately 28 kg depending on the shape of the scrap material and the resulting void in the charge (see Fig. 3).

Aluminium losses during melting can be easily compensated by charging a higher Al concentration from the start. The evaporation rate of Al at our experimental conditions was estimated based on the experimental findings of Guo et al. [13] and extrapolated to the actual crucible diameter of 25 cm at an expected holding time of

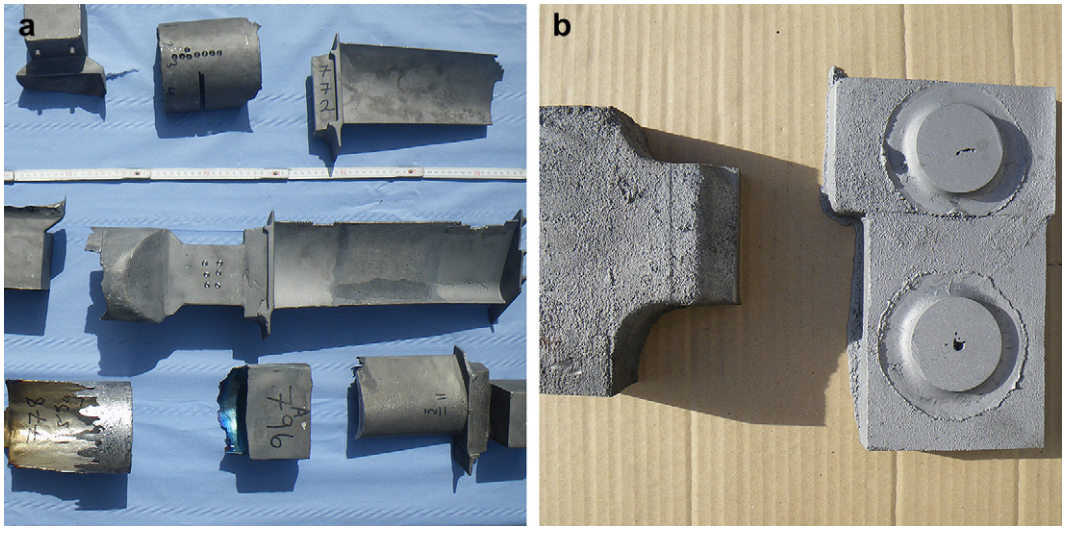

Fig. 2. Scrap from Ti46Al8Ta and Ti46Al8Nb used in trials.

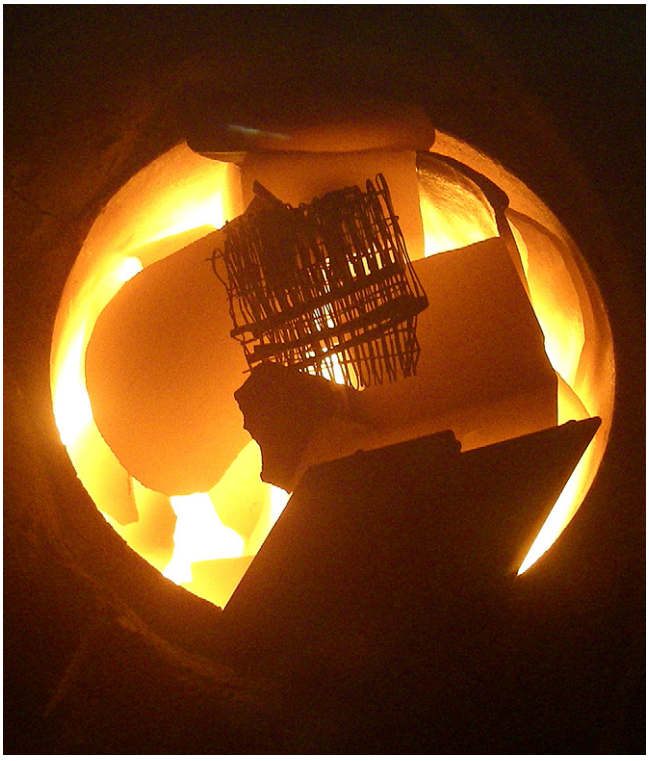

Fig. 3. Heated scrap charge prior to melting.

4500 s. Composition was adjusted by addition of 100 g Al granules for the TiAl–Nb alloy and 310 g Al for the TiAl–Ta alloy respectively. Furthermore 91 g of Ta were added to the latter. The material was charged into the crucible at room temperature, the furnace was then closed, evacuated below 1×10^{-3} mbar and flushed with argon twice in order to minimize the residual oxygen in the chamber.

Melting took place under argon to reduce the evaporation of volatile alloying constituents. To avoid thermal shocks in the crucible, melting power was increased in discrete steps every half hour. After detecting the first molten metal, power was kept constant until all material was liquid. The casting temperature was aimed at 1650–1700 °C depending on the liquidus temperature of the target alloy and measured by immersion thermocouples enclosed in a special casing. The homogeneous melt was cast into a water-cooled copper mould in order to obtain an electrode (diameter: 108 mm, length: 750 mm) with minimum segregation (Fig. 4).

2.3. Deoxidation by PESR

In order to prevent excessive calcium evaporation and allow for better control of the reducing conditions, all melts in this work were carried out in argon atmosphere at a pressure of 20 bar in a pilot-scale PESR furnace from Leybold–Heraeus (now ALD). The equipment is capable of operating at inert gas overpressures up to 50 bar, powered with a 5 kA/66 V supply and features latest monitoring and melt-control systems. Melting takes place in a tapered crucible made from copper (diameter: 178–159 mm, length: 880 mm).

Melts were carried out using an industrially available flux with 97.5% CaF_2, initial CaO-content was determined to be 1.17 wt% by a titration method. During the trials metallic calcium and virgin slag were charged into the melt through screw feeders attached to the sides of the melting furnace. The exact amount of slag and deoxidation agent charged was double-checked after the trial by mass-balancing the material leftover in the slag bunkers. Start-up

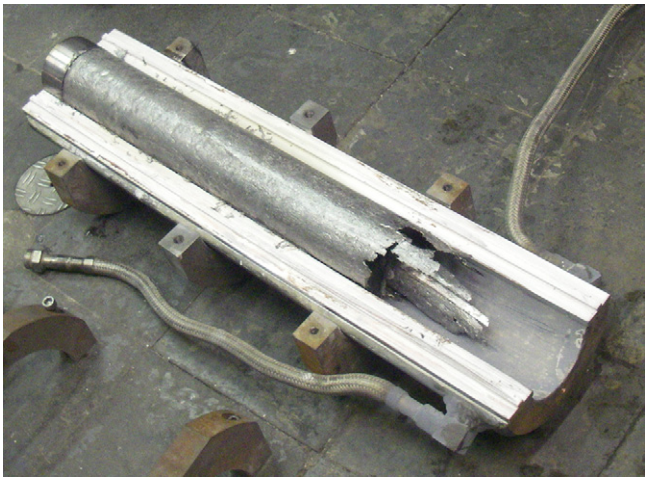

Fig. 4. VIM-cast γ-TiAl electrode in dismantled copper mould.

of the process was realised by a specially invented procedure using spent Ti50Al sputter targets for arc ignition in the slag. After the melting process, the ingot was carefully removed from the crucible. Slag samples were taken at positions corresponding to the metal samples for further investigation of slag chemistry and correlation to metal composition.

2.4. Sampling and chemical analysis

Metal samples were taken with a diamond grinding blade from both ends of the original electrode and cross sections were obtained from the PESR ingots at three different positions along the ingot axis Fig. 5) allowing to differentiate between the composition in the centre of the ingot and the outer radius. Metallic elements Ti, Al, Nb, Ta, etc. were analysed by XFA using a semi-quantitative method. Calcium was analysed by ICP, while oxygen analysis was conducted on a Ströhlein-ON mat 8500 by hot-gas extraction.

3. Theory and calculations

3.1. Chemical stability of ceramic crucibles against TiAl melts

It has been shown by various researchers, that melting of titanium alloys and titanium aluminides in particular is possible in yttria (Y_2O_3) and calcia (CaO) crucibles [14–17]. This offers best chemical

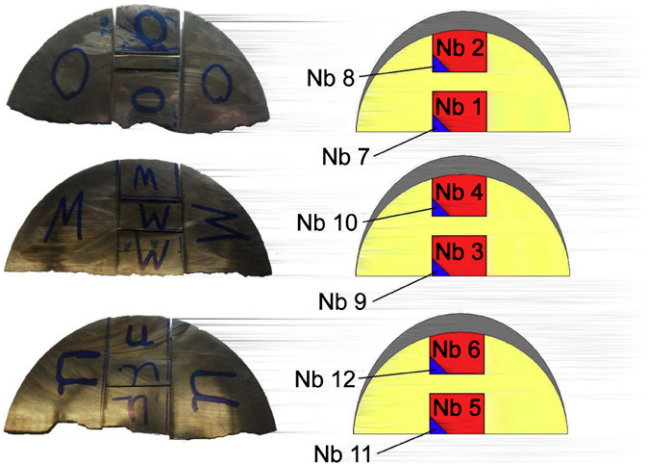

Fig. 5. Samples obtained at three different levels and two radii.

homogenisation due to inductive stirring, possibilities for composition adjustment via hot sampling and alloy charging, excellent heat control and heat distribution due to direct heating by induced eddy currents, hence a controlled evaporation of volatile elements and most important for scrap recycling a high flexibility regarding feed material (shape, dimension, number of scrap and primary materials). The application of ceramic crucibles leads to a significantly improved energy efficiency compared to melting in water-cooled "cold crucibles" made from copper, e.g. on an experimental scale of 7 kg charge weight, power requirements are reduced to 20–25 kW compared to 300 kW [17].

From the perspective of the classic Ellingham description of pure substances (Y_2O_3) and (CaO) offer the best resistance against the strongly reducing titanium melts among the oxide ceramics technically available, however activity coefficients of Ti, Y and Ca in the melt and interaction with other alloying elements have to be taken into account for a proper evaluation.

The titanium activity a_{Ti} in Ti-Al-X-melts is significantly reduced to 0.2–0.3 as compared to pure titanium melts. Furthermore melting points are about 100 °C lower for the binary γ-TiAl alloys. However a minimum oxygen pickup by attack of the crucible oxides has to be accepted. This is largely depending on the equilibrium between the melt and the crucible oxide applied, which is governed by the free enthalpy of the reaction and thus also by the superheat of the melt. It is furthermore a question of kinetics governed by wetting and melt flow if melting time is long enough to establish thermochemical equilibrium.

In a closed system the attack of the crucible material by titanium should lead to a chemical equilibrium described by Eq. (1). Thermochemical modelling was applied for a series of crucible oxides as a first step to determine this equilibrium (i.e. oxygen content of liquid metal phase) as a function of process temperature for different crucible materials [3]. For the case of melting titanium and titanium aluminides in CaO crucibles Tsukihashi et al. [15] have carried out an extensive experimental study, closely examining the Ca and O equilibria.

$$[Ca]_{Me}+[O]_{Me} \rightleftharpoons < CaO > \quad (1)$$

with $[Ca]_{Me}$ – calcium dissolved in liquid melt, $[O]_{Me}$ – oxygen dissolved in liquid melt.

As indicated in Section 3.3 Ca is expected to have a substantial vapour pressure in TiAl, thus it should be noted that calcium is continuously evaporating and thus the melt should continuously pickup oxygen without ever reaching chemical equilibrium. Evaporation kinetics in return are pressure dependent and evaporation rate is significantly reduced at the pressures VIM melting is carried out in this study (see Section 2.2). Also the reaction between the melt and the crucible itself is likely to be kinetically controlled, thus the obtained oxygen content will depend on the net change in calcium concentration based on the ratio of both these reaction speeds which should in return be controlled by the superheat of the melt.

In conclusion, lowest oxygen levels should be obtained at a minimum superheat (i.e. lowest possible diffusion coefficients, slow evaporation of calcium due to low vapour pressure), non turbulent stirring (i.e. thick boundary layers), in well filled, large, crucibles with a minimal porosity (i.e. low ratio of contact area and melt volume). It is obvious that modelling of these kinetic effects requires tremendous effort and thus experimental investigation of the matter proves to be necessary.

3.2. Metal-slag reaction in PESR

A range of suitable fluxes for the electroslag remelting of titanium alloys have been investigated thoroughly by Nafziger et al. [4] with the outcome that fluorspar (CaF_2) offers the best combination of thermochemical stability, stable processing conditions and final ingot quality. Thermochemical calculations in the system Ca–CaO–CaF_2 have shown that even the deoxidation of pure titanium should be possible by ESR using "reactive slags" where metallic calcium is added to the flux as a deoxidation agent [10]. Ca is chosen as a reactant, because of its high oxygen affinity, good solubility in the slag and available activity data [15] for the equilibrium of Ca and O in titanium melts. Furthermore Ca-reactive slags offer the removal of nitride inclusions [6]. A major challenge in the application of Ca-reactive slags for ESR however is the evaporation of Ca at the melting temperatures of the titanium alloys. This effect can be kinetically suppressed by melting under inert gas overpressure, leading to pressure electroslag remelting (PESR) as a method of choice for the deoxidation and refining of recycled titanium aluminde scrap material [10].

Dissolution of calcium from the slag into the metal phase results in a reaction at the slag metal interface according to Eq. (2). Precipitated CaO is being suspended and then dissolved in the ESR slag and hence CaO activity should be smaller than one.

$$[TiO]_{TiAl}+[Ca]_{CaF_2} \rightleftharpoons [Ti]_{TiAl}+[CaO]_{CaF_2} \quad (2)$$

with $[A]_B$ – Element A dissolved in phase B.

$$K = \frac{a(CaO)_{flux} \times a(Ti)_{metal}}{a(TiO)_{metal} \times a(Ca)_{flux}} = f(T) \quad (3)$$

with K – equilbrium constant, $a(A)_B$ – activity of A in phase B.

It becomes obvious from Eqs. 2 and 3, that through constant feeding of metal with the initial oxygen level into the metal-flux-boundary and continuous readjustment to chemical equilibrium, the flux enriches in CaO during the melt and is being depleted in Ca as the process proceeds. This has severe implications on the chemistry of the ESR process: In order to ensure a uniform oxygen content with respect to the full length of an ingot, calcium has to be added at the exactly correct rate in order to compensate for the increasing CaO-activity. Intensive thermochemical modelling of the metal slag reaction was applied by Stoephasius et al. [10] in order to allow for a controlled deoxidation by ESR. Based on a target oxygen concentration in the metal of 500 ppm, the necessary Ca-activity on the flux can be calculated for every level of CaO-activity as shown in Fig. 6.

Due to the current lack of reliable methods for online-surveillance of the activities of Ca and CaO in the slag, a process model was introduced based on mass-balance calculations that include dissolution of Ca in the metal, pressure dependent evaporation of Ca from the flux and the described deoxidation equilibrium Eq. (3).

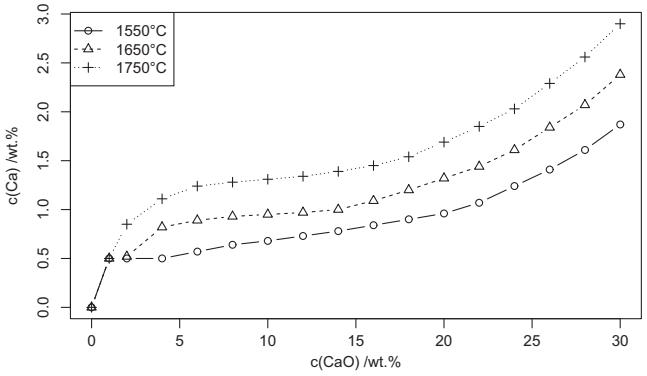

Fig. 6. Necessary Ca content in the active slag as a function of CaO concentration to reach 480 ppm oxygen in a Ti50Al melt.

This was put in to practice as a spreadsheet which can be adjusted to melting parameters, e.g. metal melt rate, initial oxygen level of the metal, operating pressure etc. which calculates feedrates for both calcium compensation and feeding of virgin slag.

3.3. Evaporation of calcium during VAR

When VAR is operated under vacuum at pressures below 1×10^{-3} mbar the evaporation of excessive Ca from TiAl should be possible in analogy to the removal of magnesium from titanium sponge upon constitutional melting in the same process. Modelling of the thermochemistry and kinetics of this evaporation reaction is however difficult due to the lack of activity data for Ca in a TiAl melt. For the following model calculation, the dissolution of Ca was therefore assumed to be ideal (Raoult's law) in first approximation. As a result Ca vapour pressure remains a function of temperature through the standard vapour pressure above a virtual pure calcium melt and of the mole fraction of Ca dissolved.

While the evaporation of basically all residing calcium should be feasible from a thermochemical standpoint, it has to be considered, that evaporation in vacuum is a kinetically controlled process. It is an intrinsic characteristic of VAR that only a partial volume of the total metal is molten at a time. Thus the final Ca concentration of a TiAl ingot after refining by VAR is a function of the kinetics of evaporation and of the metal melt rate which governs mass of the molten pool. The Langmuir Eq. (4) describes the general kinetics of evaporation across the liquid phase boundary into the vacuum and allows an estimation of the net distillation mass flow for a given vapour pressure of calcium in the metal melt.

$$j = \alpha \cdot \frac{1}{\sqrt{2 \cdot \Pi \cdot M_{Ca} \cdot R \cdot T}} \cdot \left(p_{Ca,sat} - p_{Ca,act} \right) \quad (4)$$

where j = net mass flow of evaporation [mol/m^2 s], α - distillation coefficient [−].

For distillation of metal melts, the distillation coefficient is usually set to 1 for free evaporation under vacuum. This gives a peak evaporation rate of 2.985 mol m^{-2} s (119.7 g m^{-2} s) for a Ti50Al-melt at 1550 °C with an initial Ca concentration of 1500 ppm which can be expected after deoxidation by PESR or direct deoxidation in VIM. In VAR, the evaporating surface is represented by an annular gap between the electrode and the mould walls. For the experimental set-up available this translates to a maximum Ca evaporation rate of 1.269 g s^{-1}. However, with decreasing concentration, the vapour pressure of Ca decreases and so does the mass flow. Fig. 7 shows the dependency of Ca evaporation rate on the concentration and the necessary time to reach a certain degree of refining for a mass of 100 g of melt. It becomes apparent that an almost complete removal of Ca should be achieved in 0.66 s which translates to a maximum melt rate of 9.09 kg min^{-1}.

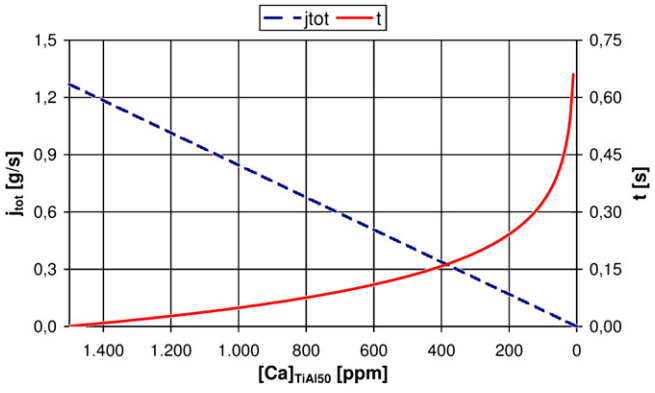

Fig. 7. Calculated mass flow of calcium evaporation and minimum holding time for removal of 1500 ppm Ca from 100 g Ti50Al.

4. Results

4.1. Vacuum induction melting and casting

In our melting campaigns, the special CaO crucibles applied for VIM lasted about five melts before they had to be replaced. Main reason for replacement are cracks in the sidewalls at melt level due to forming of oxide layers there. Special crucible care was not applied, so that in production scale a significantly increased lifetime can be expected.

The results obtained after melting and casting of two electrodes of Ti46Al8Ta and T46Al8Nb are shown in Table 1. The anticipated composition presented here is based on the average analysis of the original scrap charge and takes into account Al evaporation as well as composition adjustment by charging Al granules and Ta scrap as described in Section 3.1. In can be observed that alloying of both Al and Ta could be successfully conducted compared to the initial alloy. The results however show significantly higher Al levels than expected and consequently Ta and Nb concentration in both alloys appear to be slightly below target. Possible reasons for this deviation are discussed below in Section 5.

Oxygen levels in the Ti46Al8Ta electrode were determined to be 1874 ppm at the top vs. 1454 ppm at the bottom side of the casting and 3620 ppm−2332 ppm respectively in the Ti46Al8Nb electrode. This goes in hand with a second observation that Yttrium was detected at the top of each casting (1450 ppm in the Ta-alloy and 2860 ppm in the Nb-alloy) but was not detectable at the bottom, and neither in the later obtained PESR ingots after remelting. Possibly Yttria particles from the face coating applied to the mould walls could detach upon casting and float on the not yet solidified TiAl melt while solidification takes place from bottom to top. It can further be discussed whether there is a segregation mechanism for dissolved oxygen in the melt or if CaO particles precipitate upon cooling and float in analogy to the Yttria particles.

The Ti46Al8Ta-alloy shows a 350 ppm contamination by Zr, which was detected before in some of the delivered castings and originates from Zirconia components of the shell mould system. Zr contamination could be traced also to the PESR ingots and it appears that there is no change in concentration i.e. removal of Zr by PESR, as can be expected. A contamination by Fe 1430 ppm, Si 895 ppm and Mo 735 ppm could be detected on the Nb-alloy but not in the Ta-alloy and was most likely obtained from residual mould material on the rough surface of the scrap pieces.

Segregation of Ti could be observed in the cast VIM electrodes with slightly decreasing levels from bottom to top of the electrode, while Al concentrations show the exactly opposite trend as expected. Note that in Fig. 9 the *x*-axis measures from the bottom of the PESR ingot to the top of the ingot. Because of the top-down melting practice applied, the top section of the cast VIM electrode

Table 1
Results of adjusted alloy composition after VIM for Ti46Al8Ta (above) and Ti46Al8Nb (below).

In at.%	Ti	Al	Ta
Ti46Al8Ta			
Composition of scrap	45.85	46.30	7.65
Anticipated composition	45.99	46.01	8.00
Obtained analysis	44.34	47.80	7.76
Ti46Al8Nb			
Composition of scrap	48.18	43.48	8.24
Anticipated composition	47.95	43.85	8.20
Obtained analysis	46.62	45.13	7.69

corresponds to the bottom of the ingot and the electrode bottom corresponds to the ingot top. The segregation of both Ti and Al appears to be more pronounced in the electrode obtained from the Ta-alloy. This is however not directly connected to the segregation of Nb and Ta which is similar. Nb concentration increases from 7.60 at% at the electrode bottom to 7.78 at% at the top of the electrode while Ta segregates similarly from 7.67 at% at the bottom to 7.84 at.% at the top.

4.2. Pressure electroslag remelting

Low oxygen levels < 500 ppm were achieved in all samples obtained from the ingots, with an average oxygen level at 244 ppm. Fig. 8 shows that the analysed oxygen and calcium concentrations are in good agreement to the model of the solubility products we obtained from the experimental study by Tsukihashi et al. [15].

Ti and Al segregation observed in the cast electrodes was smoothed by the backmixing-effect in PESR and differences in concentration between center and radius section of the ingot appear to be at an acceptable level of approx. 0.5 at%. For both Nb and Ta significant differences between center and radius can be observed in the bottom part of the ingot and are probably due to transient melting conditions at his stage. Concentration of these ternary elements picks-up to electrode level during stationary melting with significantly reduced difference between center and radius.

5. Discussion

The effects of composition adjustment during VIM by charging of Al granules and Ta sheet could be clearly observed and desired target analysis was nearly met at first melt with minor deviations in Al content. An overcharging of Al can be avoided by proper calculation or empirical determination of the evaporation rate for Al. A second very important input in composition adjustment is statistically sound sampling of a potentially inhomogeneous scrap charge. This does not only refer to the quantity of samples but also to the method for bulk analysis. The impurities Fe, Si and Mo found in the cast electrodes from the Nb-alloy were initially not detected in the XFA cross sections from the bulk scrap but may have their origin on the outer surface of the scrap. Scrap from the Ta-alloy was sandblasted and showed clean and smooth surfaces while the Nb-alloy pieces had a rough surface even after sandblasting and might have still contained oxides from the shell mould system. Probability for a contamination from the crucible itself is very low in our case due to application of high purity CaO crucibles. This is underlined by the fact that Ta-alloy was the first casting to be made from the virgin crucible yet aforementioned contaminations were not found in this first electrode. The analysis of the second casting, the Nb-alloy shows nearly 0.9 wt% Ta and indicates that on potential production level alloy change should be avoided and different alloy scraps should be melted in campaigns.

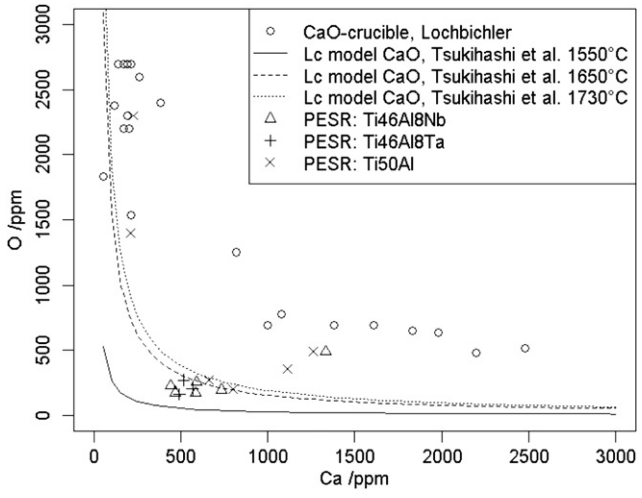

Fig. 8. Low oxygen obtained in PESR melted TiAl alloys vs. modelled solubility product L_c obtained from literature [15].

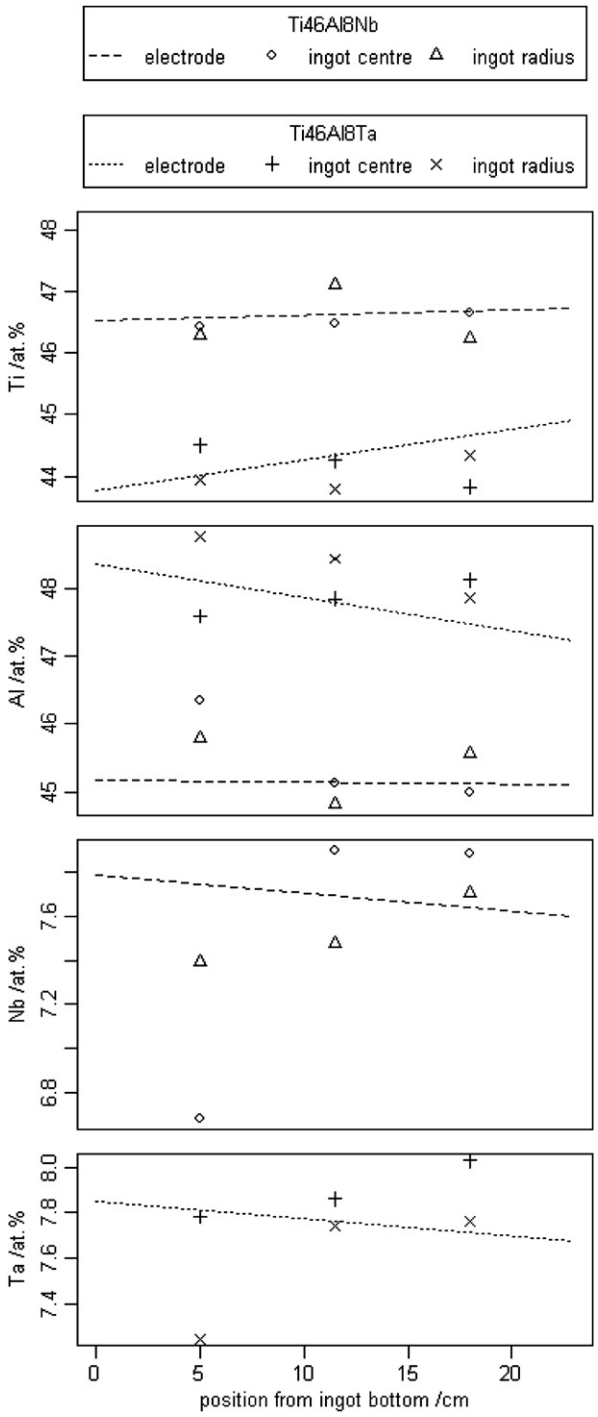

Fig. 9. Macrosegregation of Ti, Al and Nb/Ta after VIM casting and in obtained PESR ingots.

The obtained oxygen levels in the PESR ingots are highly reliable with mean errors below 10% upon triple analysis. This however does not hold for the determination of calcium concentration. A detection of calcium below 800 ppm by XFA is questionable because of the high signal to background noise ratios and the alternative to dissolve TiAl in acid for ICP analysis results in a relatively large mean error of 60%. This is due to the fact that HF is a necessary component for dissolution of the sample but should be kept to a minimum as the solubility product for CaF_2 is so low that dissolved Ca precipitates as fluoride which leads to an analytical error. However within the achievable accuracy, the obtained results for the CaO equilibrium fit very well to the theoretical expectations.

6. Conclusions

The recycling of γ-TiAl alloys by consolidative melting via VIM in a CaO crucible and subsequent deoxidation by PESR has been demonstrated to prove the high potential of such a process chain. Alloy composition was successfully adjusted and the major process mechanisms are understood. A correct sampling of scrap charges in a statistical meaningful manner and a unified standard for chemical analysis of TiAl are to be improved in order to obtain a more precise control of alloy composition and impurity content as necessary for the sensitive TiAl alloys.

PESR offers efficient deoxidation of TiAl even down to 250 ppm if correctly controlled. This offers an interesting starting point for reuse of the material and might reveal so far unseen material properties. Macrosegregation in the obtained ingots is minimal and segregation effects from the VIM cast electrodes could be homogenised by PESR. After the first two processing steps, the material contains residual Ca in a concentration of 500–1000 ppm which is probably too much for direct reuse in an investment casting process due to strong evaporation tendencies. However calculations indicate that it should be completely removed by subsequent VAR and trials on the obtained material will be carried out in the near future for experimental proof.

Acknowledgements

The presented experimental works were carried out in the framework of the EU FP6 project IMPRESS (contract number NMP3-CT-2004-500635). The authors would like to thank the European commission for funding of their work, as well as the German ministry of education and research (BMBF) and the Deutsche Forschungsgemeinschaft (DFG) who delivered funding for elaboration of the basic principles of the presented work in earlier projects. We would further like to acknowledge the support of GfE Gesellschaft für Elektrometallurgie mbH, Nürnberg, Germany, ACCESS e.V., Aachen, Germany, IRC Birmingham, UK and Doncasters Settas, Jumet, Belgium for providing scrap material for trials on TiAl recycling. The authors gratefully acknowledge the support of ACCESS e.V., Aachen, Germany for assistance in preparation and interpretation REM micrographs.

References

[1] Hammerschmidt J. Entwicklung einer prozessroute zur herstellung von gamma-tial-legierungen durch aluminothermie und schutzgas-elektroschlackeumschmelzen. IME Metallurgische Prozesstechnik und Metallrecycling, RWTH Aachen University; 2003, Ph.D. thesis.
[2] Stoephasius J. Elektroschlackeraffination aluminothermisch hergestellter gamma-titanaluminide. IME Metallurgische Prozesstechnik und Metallrecycling, RWTH Aachen University; 2006, Ph.D. thesis.
[3] Morscheiser J, Friedrich B, Lochbichler C, Aachen. Potential of ceramic crucibles for melting of titanium-alloys and gamma-titaniumaluminde. Proceedings of the 51st international colloquium on refractories. 978-3-00-025895-4. Forschungsgemeinschaft Feuerfest e.V; 2008.
[4] Nafziger R. Slag compositions for titanium electroslag remelting; 1969. Second international symposium on electroslag remelting technology.
[5] Armantrout C, Nafziger R. Proceedings of the seventy-third annual meeting of the American foundryman's society. Development of electroslag melting technique for titanium: selected properties of fabricated material, vol. 77; 1969. pp. 353–359.
[6] Benz M, Ryabtsev A. ESR as a fast technique to dissolve nitrogen rich inclusions in titanium. Materials Research Innovations; 1999:364–8.
[7] Nafziger R. Electroslag melting of titanium and aluminium. The Electroslag remelting process. U.S. Dept. of the Interior, Bureau of Mines; 1976.
[8] Choudhury A, Scholz H, Ludwid N. Electroslag remelting of titanium. Conference proceedings; 1993.
[9] Paton B, Medovar B, Benz M, Nafziger R, Medovar L. Esr for titanium: yesterday, today, tomorrow. 9th world conference on titanium. St. Petersburg; 1999.
[10] Stoephasius J, Reitz J, Friedrich B. ESR refining potential for titanium alloys using a CaF_2-based active slag. Advanced Engineering Materials 2007;9. doi:10.1002/adem.200700009.
[11] Reitz J, Stoephasius J, Friedrich B. Tracing ca and f during remelting of titanium-aluminides in ESR and VAR. Titanium 2009 – conference proceedings. International titanium association. In: Association I.T, editor, editor; 2009.
[12] Jarvis D, Voss D. Impress integrated project–an overview paper. Materials Science and Engineering A 2005;413–414:583–91.
[13] Guo J, Jia J, Liu Y, Liu G, Su Y, Ding H. Evaporation behavior of aluminum during the cold crucible induction skull melting of titanium aluminum alloys. Metallurgical and Materials Transactions B 2000;31(4):837–44.
[14] Kobayashi Y, Tsukihashi F. Thermodynamics of yttrium and oxygen in molten Ti, Ti_3Al, and TiAl. Metallurgical and Materials Transactions B 1998;29(5):1037–42.
[15] Tsukihashi F, Hatta T, Tawara E. Thermodynamics of calcium and oxygen in molten titanium and titanium–aluminum alloy. Metallurgical and Materials Transactions B 1996;27(6):967–72.
[16] Renjie C, Ming G, Hu Z, Shengkai G. Interactions between TiAl alloys and yttria refractory material in casting process. Journal of Materials Processing Technology 2010;210(9):1190–6.
[17] Sakamoto K, Yoshikawa K, Kusamichi T, Onoye T. Changes in oxygen contents of titanium aluminides by vaccum induction, cold crucible induction and electron beam melting. ISIJ International 1992;32(5).